



Voxel-based morphometry and histological analysis for evaluating hippocampal damage in a rat model of cardiopulmonary resuscitation



Hideaki Suzuki ^{a,*}, Akira Sumiyoshi ^b, Yasuyuki Taki ^{c,d,e}, Yasuharu Matsumoto ^a, Yoshihiro Fukumoto ^a, Ryuta Kawashima ^{b,d,f}, Hiroaki Shimokawa ^a

^a Department of Cardiovascular Medicine, Tohoku University Graduate School of Medicine, Sendai, Japan

^b Department of Functional Brain Imaging, Institute of Development, Aging and Cancer, Tohoku University, Sendai, Japan

^c Division of Medical Image Analysis, Department of Community Medical Supports, Tohoku Medical Megabank Organization, Tohoku University, Japan

^d Division of Developmental Cognitive Neuroscience Institute of Development, Aging and Cancer, Tohoku University, Japan

^e Department of Radiology and Nuclear Medicine, Institute of Development, Aging and Cancer, Tohoku University, Japan

^f Department of Advanced Brain Science, Institute of Development, Aging and Cancer, Tohoku University, Sendai, Japan

ARTICLE INFO

Article history:

Accepted 14 March 2013

Available online 2 April 2013

Keywords:

Voxel based morphometry

Brain histology

Animal model

Hippocampus

Cardiopulmonary resuscitation

ABSTRACT

Cardiac arrest and subsequent cardiopulmonary resuscitation (CPR) induce hippocampal damage, which has been identified using histological analysis of post-mortem brains. Voxel-based morphometry (VBM), an in-vivo assessment of regional differences in the concentration or volume of a particular tissue such as gray matter, has revealed CPR-induced decreases in gray matter in the hippocampus, where histopathological findings were observed. However, the potential link between the changes in gray matter detected by VBM and hippocampal damage has not been investigated directly. In this study, we compared results obtained using VBM directly to results from histological analyses in the same CPR rat brains, which exhibited neuronal loss and microglial invasion in the CA1 region of the hippocampus (CA1). T2-weighted images were obtained and preprocessed for VBM to produce gray matter concentration (GMC) maps in rats with asphyxia-induced cardiac arrest and CPR and sham-operated controls ($n = 12$ each). Brains were fixed, and the number of neurons and microglia in CA1 were counted. VBM revealed a significant decrease in GMC in CPR rats compared to sham-operated controls. The CPR-induced decrease in GMC was localized to CA1, which is the same brain region where neuronal loss and microglial invasion were noted in response to CPR. GMC values were positively correlated with the number of neurons and tended to be negatively correlated with the number of microglia in CA1 of CPR rats. In conclusion, these results indicate that VBM-detected alterations in gray matter can be used as a surrogate marker for hippocampal damage following CPR.

© 2013 Elsevier Inc. All rights reserved.

Introduction

Sudden cardiac arrest is a disastrous situation that results in death without immediate efforts of cardiopulmonary resuscitation (CPR). One of the most significant problems reported by survivors after CPR is the complication of long-term neurological and cognitive deficits (Lim et al., 2004; Mateen et al., 2011; Roine et al., 1993) that can result from damage to gray matter regions of the brain that are vulnerable to hypoxia, such as the hippocampus (Cummings et al., 1984; Horstmann et al., 2010; Press et al., 1989; Volpe and Petito, 1985; Zola-Morgan et al., 1986). Hippocampal damage following CPR has been originally identified using histological analysis of post-mortem brains (Cummings et al., 1984; Press et al., 1989; Volpe and Petito, 1985; Zola-Morgan et al., 1986). More recently, voxel-based morphometry (VBM), an unbiased

objective technique based on magnetic resonance imaging (MRI), has been used to assess regional differences in the concentration or volume of a particular tissue such as gray matter in animals and humans (Ashburner and Friston, 2000, 2001; Biedermann et al., 2012; Quallo et al., 2009; Sawiak et al., 2009; Yang et al., 2011). In survivors after CPR, VBM has revealed decreases in gray matter in several brain regions, including the hippocampus (Horstmann et al., 2010), where histopathological findings were observed. However, the potential link between the changes in gray matter detected by VBM and CPR-induced hippocampal damage has not been investigated directly.

A rat model of cardiac arrest and subsequent CPR has been shown to be useful in investigating the mechanisms underlying CPR-induced brain damage (Empey et al., 2012; Katz et al., 1995; Keilhoff et al., 2010, 2011; Liu et al., 2012; Shoykhet et al., 2012). Studies using this model have revealed cellular events in the hippocampus that are similar to those observed in humans, such as neuronal cell death and microglial invasion in the CA1 region of the hippocampus (CA1) (Katz et al., 1995; Keilhoff et al., 2010, 2011; Shoykhet et al., 2012). However, VBM has not revealed CPR-induced alterations in gray

* Corresponding author at: Department of Cardiovascular Medicine, Tohoku University Graduate School of Medicine, 1-1, Seiryomachi, Aoba-ku, Sendai, 980-8574, Japan. Fax: +81 22 717 7156.

E-mail address: hd.suzuki.1870031@cardio.med.tohoku.ac.jp (H. Suzuki).

matter in rats. We previously reported an in-vivo rat T2 MRI template that includes three classes of probability segmentations, which enables us to perform VBM on rat brains (Valdés-Hernández et al., 2011). In animal VBM studies, it is possible to use histological analyses of post-mortem brains to validate VBM-detected gray matter changes. In the present study, we compared results obtained using VBM directly to results from histological analyses of CA1 in the same CPR rat brains. The purpose is to investigate whether VBM-detected alterations in gray matter can be used as a surrogate marker for hippocampal damage in CPR rats. The hypotheses are as follows: (1) CPR induces gray matter changes that can be detected by VBM in brain regions including CA1, and (2) the gray matter changes detected by VBM are associated with the number of neurons and/or microglia in CA1.

Materials and methods

Animals

A total of 24 male Sprague–Dawley rats (11 week-old; SLC, Shizuoka, Japan) were assigned to either the CPR group or the sham-operated group, which received anesthesia and vessel cannulations but not cardiac arrest ($n = 12$ each). No significant differences in the body weight were observed in CPR (365 ± 7 g) and sham-operated rats (362 ± 7 g) ($P = 0.731$). All procedures and protocols were performed in accordance with the policies established by the Animal Care Committee at Tohoku University, Sendai, Japan (approval number: 2012-241).

The CPR rats

CPR rats were subjected to cardiac arrest and a subsequent CPR protocol that has been described previously (Empey et al., 2012; Katz et al., 1995; Keilhoff et al., 2010, 2011; Liu et al., 2012; Shoykhet et al., 2012). Rats were anesthetized with isoflurane, and were placed in the prone position on a hotplate (AS ONE, Osaka, Japan) to maintain their rectal temperature at 37.0 ± 1.0 °C throughout the entire procedure as monitored using a thermometer (Unique Medical Co., Ltd., Tokyo, Japan). Surgical preparations were performed under 3% isoflurane as follows. Polyethylene catheters were inserted into the femoral artery and vein for examining arterial blood pressure and systemic drug delivery, respectively. Blood pressure waves transmitted from the arterial polyethylene catheter were digitized by a pressure transducer (DTXPlus™, BD, Franklin Lakes, NJ, USA), amplified by an MEG-6108 amplifier (Nihon Kohden Corporation, Tokyo, Japan), and analyzed by a PowerLab/16SP and LabChart 6 device (ADInstruments, Inc., Colorado Springs, CO, USA). Subsequently, rats were orally intubated, mechanical ventilation was initiated at a respiration rate of 50 breaths/min by a ventilator (Harvard Apparatus, Holliston, MA, USA), and isoflurane was washed out with room-air for 5 min after the intravenous administration of vecuronium (2 mg/kg) for immobilization. After the 5-min washout, asphyxia was induced by disconnecting the ventilator and plugging the tracheal tube, which resulted in cardiac arrest within approximately 4 min (Fig. 1). After 8 min of this apnea and airway obstruction, CPR was initiated by starting mechanical ventilation with 100% O₂ at a frequency of 50 breaths/min, administering epinephrine (0.02 mg/kg) followed by sodium bicarbonate (1 mmol/kg) intravenously, and applying sternal compression at a rate of 200/min until restoration of spontaneous circulation (ROSC) was achieved. CPR was stopped if ROSC was not obtained within 2 min. At 60 min after the start of CPR, ventilation was withdrawn, extubation was performed with no reversal medication for vecuronium, the catheters were removed, the vessels were ligated, and the skin was closed. The CPR rats were returned to their cages where they were housed for 4 weeks in a room on a 12-h light–dark cycle until the time of MRI recordings.

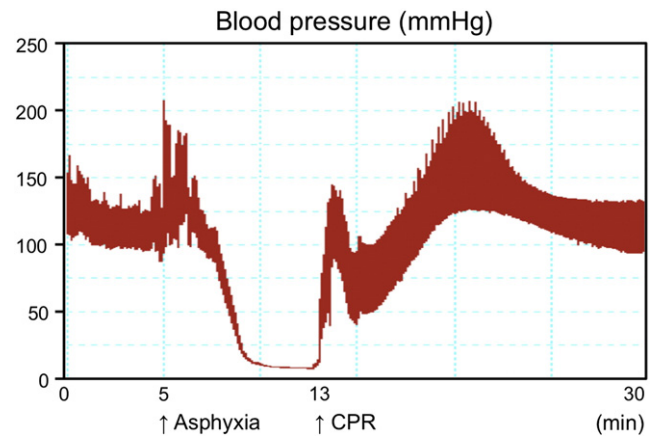


Fig. 1. A representative image of blood pressure monitoring during the cardiac arrest and subsequent CPR protocol. CPR, cardiopulmonary resuscitation.

MRI recordings

Four weeks after the CPR or sham protocol, T2 anatomical MRI images for VBM were obtained from CPR and sham-operated rats ($n = 12$ each, 429 ± 11 g and 456 ± 11 g, respectively, $P = 0.083$). Subsequent animal preparations for MRI recordings were performed as described in our previous studies (Sumiyoshi et al., 2012). Briefly, rats were initially anesthetized with isoflurane, and polyethylene catheters were inserted into the femoral artery and vein to examine blood pressure and systemic drug delivery, respectively. The rats were orally intubated for artificial ventilation, were placed in the prone position on a custom-built MRI bed with a bite bar, and mechanically ventilated at a respiration rate of 60 ± 1 breaths/min using a ventilator (SAR-830/AP, CWE Inc., Ardmore, PA, USA). After the rats received a bolus injection of pancronium (2 mg/kg), anesthesia was maintained with 1.5% isoflurane and the continuous administration of pancronium (2 mg/kg/h).

All MRI data were acquired using a 7.0-T Bruker PharmaScan system (Bruker BioSpin, Ettlingen, Germany) with a 38-mm-diameter bird-cage coil. Prior to all MRI acquisitions, we first performed global magnetic field shimming inside the core and later completed it at the region of interest (ROI) using a point resolved spectroscopy protocol (Sumiyoshi et al., 2012). The line width (full width at half maximum) at the end of the shimming procedure ranged from 10 to 16 Hz in the ROI (approximately 300 μ m). T2-weighted images (T2WI) were obtained using a 2D-RARE sequence with the following parameters: TR = 4600 ms, TE_{eff} = 30 ms, RARE factor = 4, SBW = 100 kHz, flip angle = 90°, FOV = 32 × 32 mm², matrix size = 256 × 256, voxel size = 125 × 125 μ m², number of slices = 54, slice thickness = 0.5 mm, slice gap = 0 mm, and number of repetitions = 10.

VBM analysis

All T2WIs were analyzed using the statistical parametric mapping software (SPM8, Wellcome Department of Cognitive Neurology, London, UK) and custom-written software in MATLAB (MathWorks Inc., Natick, MA, USA). In the present study, VBM was performed using a method that was modified as previously applied in humans (Taki et al., 2012). First, the T2WIs were resized by a factor of 10 (Biedermann et al., 2012) and were realigned and resliced to adjust for head motion. The realigned anatomical images were then averaged to produce mean images. Second, after the mean images were aligned with the Wistar rat template brain (Valdés-Hernández et al., 2011), they were segmented into images of gray matter (GM), white matter (WM) and cerebrospinal fluid (CSF) by applying a unified segmentation approach (Ashburner



Fig. 2. The population specific template (A, B) and probability maps for gray matter (C, D), white matter (E, F), and cerebrospinal fluid (G, H) tissue classes. Each voxel of the probability maps is colored according to its probability values for its tissue classes (i.e., gray matter, white matter or cerebrospinal fluid).

and Friston, 2005) using the probabilistic maps of the Wistar rat brain (Valdés-Hernández et al., 2011). The obtained GM, WM and CSF images and T2WIs were rigid-body aligned (3 rotations and 3 translations) to the Wistar rat brain template (Valdés-Hernández et al., 2011) and were resampled into 1.25 mm (for the resized images) isotropic voxels. Third, the aligned GM, WM and CSF images were used to create a customized, more population-specific template (Fig. 2) using diffeomorphic

anatomical registration using exponentiated lie algebra (DARTEL) template-creation tool (Ashburner, 2007). DARTEL has been shown to produce a more accurate registration than the standard VBM procedure (Klein et al., 2009) and is potentially suitable for performing VBM using probability maps from different rat strains. Fourth, each rat's gray matter image was warped using its corresponding smooth, reversible deformation parameters to transform it to the custom template space and then

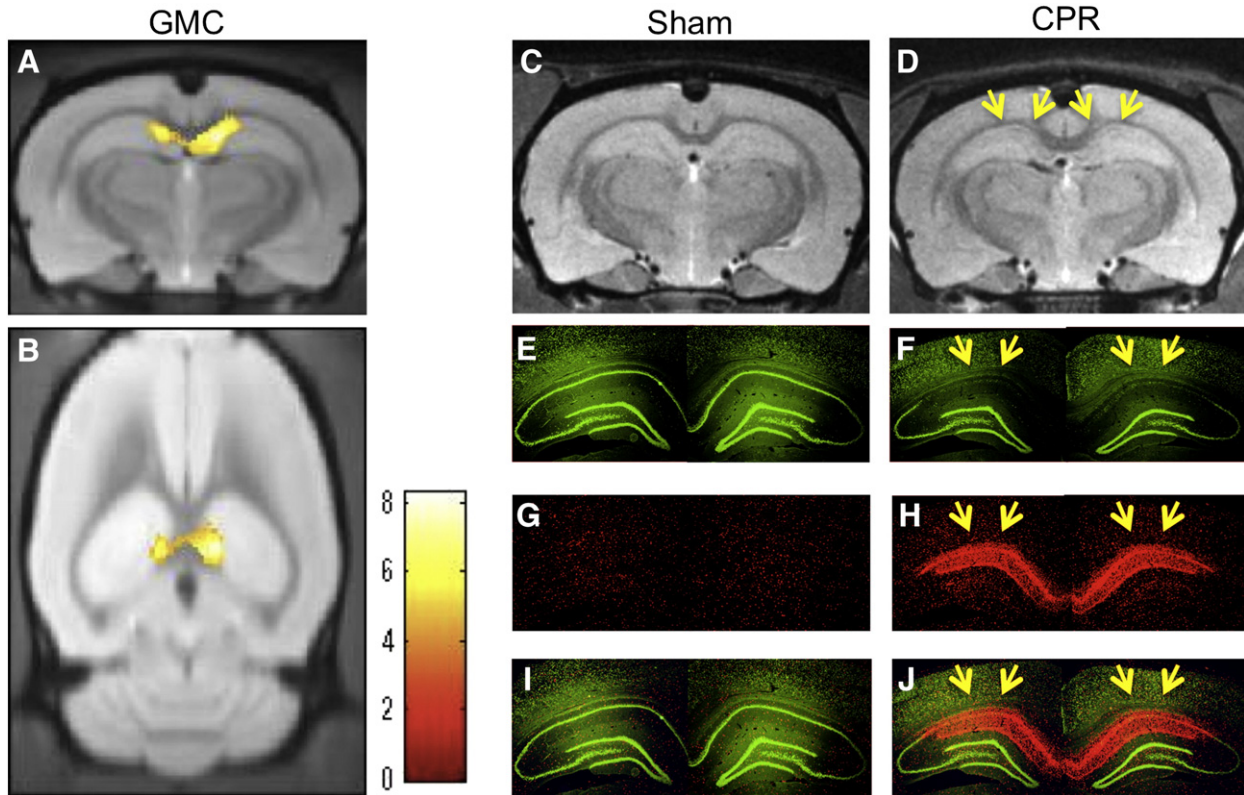


Fig. 3. VBM results, T2WI and immunohistochemical images comparing CPR rats to sham-operated controls. A, B) Significant regional GMC decrease in CPR rats compared to sham-operated controls. The results were displayed on the custom template that included both groups. The color calibration bars represent the critical T-score magnitudes with a threshold level of $P < 0.05$ FDR corrected. The center of the GMC decrease was exceeded at $P < 0.05$ FWE corrected. C–J) Representative pictures showing T2WI (C, D), staining with a neuronal marker (Neu-N, Green, E, F), and staining with a microglial marker (Iba-1, Red, G, H), and merged images depicting double labeling with neuronal and microglial markers (I, J). Yellow arrows indicate CA1. The images in C, E, G and I were taken from a single sham-operated control, and the images in D, F, H and J were obtained from a single CPR rat. CA1, CA1 region of the hippocampus; CPR, cardiopulmonary resuscitation; FDR corrected, corrected for multiple comparisons using the false discovery rate method; FWE corrected, corrected for multiple comparisons using the family wise error method; GMC, gray matter concentration; T2WI, T2 weighted image; VBM, voxel based morphometry.

Table 1

Decreases in gray matter concentration in CPR rats compared to the sham-operated controls.

	Coordinates (x, y, z)	Z score	Voxels in cluster
Hippocampus	(1.44, 3.14, -3.6)	5.53	1991

Coordinates are relative to bregma in the medial–lateral (x), superior–inferior (y), and anterior–posterior (z) directions (mm). Voxels in cluster are expressed as the number of voxels exceeding the threshold of $P < 0.05$ corrected for multiple comparisons using the false-discovery error method. CPR, cardiopulmonary resuscitation.

to the Wistar rat template space. Fifth, the warped gray matter images were unmodulated or modulated to correct for volume changes that may have occurred during nonlinear normalization by calculating Jacobian determinants derived from spatial normalization steps and multiplying each voxel by the relative change in volume to obtain the gray matter volume (Good et al., 2001). Finally, the warped unmodulated or modulated gray matter images were smoothed with an isotropic Gaussian kernel to produce gray matter concentration (GMC) or gray matter volume (GMV) maps respectively by convolving an 8-mm (for the resized images) full-width at half maximum. Note that, although the image preprocessing was performed in the resized scales, the results of VBM analysis were displayed in the original scales.

Histological analysis

After MRI recordings, all the rats were transcardially perfused first with phosphate buffered saline (PBS, pH 7.4) and then with paraformaldehyde in PBS (4% PFA). The brains were carefully removed from the skull, post-fixed in 4% PFA, and embedded in paraffin. Consecutive 3- μ m coronal sections were obtained from approximately bregma -3.6 mm, which includes the focus of the regional GMC decrease

observed in CPR rats compared to sham-operated controls (Figs. 3C, D, Table 1). These sections were incubated with mouse anti-NeuN (neuronal nuclei, 1:500; Chemicon), a neuronal marker, and rabbit anti-Iba1 (ionized calcium binding adaptor molecule 1, 1:500; Wako Pure Chemical Industries, Ltd.), a microglial marker, and were examined using a fluorescence microscope (BZ-9000, Keyence Corporation, Osaka, Japan). The number of neurons and microglia in CA1 in each section was counted inside a microscopic field (Taguchi et al., 2012), which was at 200 \times magnification ($540 \times 720 \mu\text{m}$) and was positioned near the focus of the significant regional GMC decrease in CA1 observed in CPR rats compared to sham-operated controls (Fig. 4A).

Statistical analysis

To reveal regional changes in gray matter due to cardiac arrest and subsequent CPR, the GMC and GMV maps of CPR rats were compared to those obtained from sham-operated controls using a Student's *t*-test at each voxel. We excluded all voxels with a gray matter probability value below 0.2 to include only voxels with sufficient gray matter proportion and avoid possible edge effects between gray matter and white matter or cerebrospinal fluid (May et al., 2007). The significance level was first set at $P < 0.05$ and was corrected for multiple comparisons by using the family-wise error method (FWE corrected) for both GMC and GMV analyses. Second, less stringent threshold of $P < 0.05$ corrected for multiple comparisons by using the false-discovery rate method (FDR corrected) with a minimum cluster size of 200 voxels was applied to GMC analysis. A significant cluster of differences in GMC ($P < 0.05$ FDR corrected with a minimum cluster size of 200 voxels) was localized inside CA1 (Figs. 3C, D), which was thus considered a region of interest (ROI) and subjected to the following correlation analyses (Zhang et al., 2011).

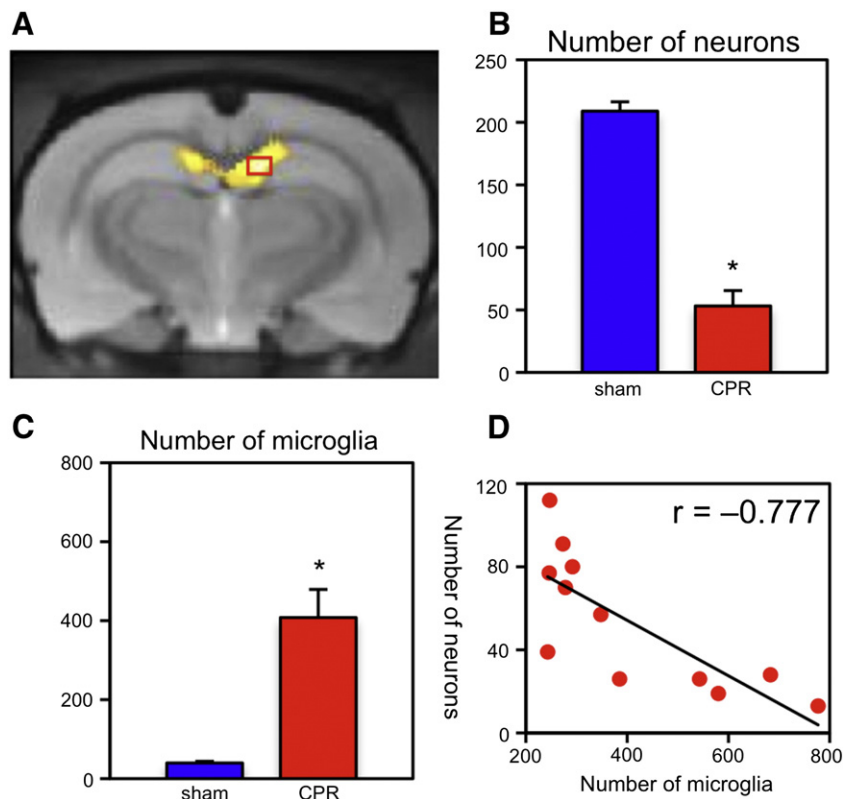


Fig. 4. Quantification of the number of neurons or microglia in CA1 in CPR rats and sham-operated controls. A) The number of neurons or microglia in each rat was examined inside the red rectangle ($540 \times 720 \mu\text{m}$) near the focus of the significant regional GMC decrease in CA1 in CPR rats compared to sham-operated controls (Fig. 2A, B, Table). B) The number of neurons in CA1 in CPR rats compared to sham-operated controls. C) The number of microglia in CA1 in CPR rats compared to sham-operated controls. D) A correlation between the number of neurons and microglia in CA1 in CPR rats. * $P < 0.001$ compared to sham-operated controls. CA1, CA1 region of the hippocampus; CPR, cardiopulmonary resuscitation; GMC, gray matter concentration; sham, sham operation.

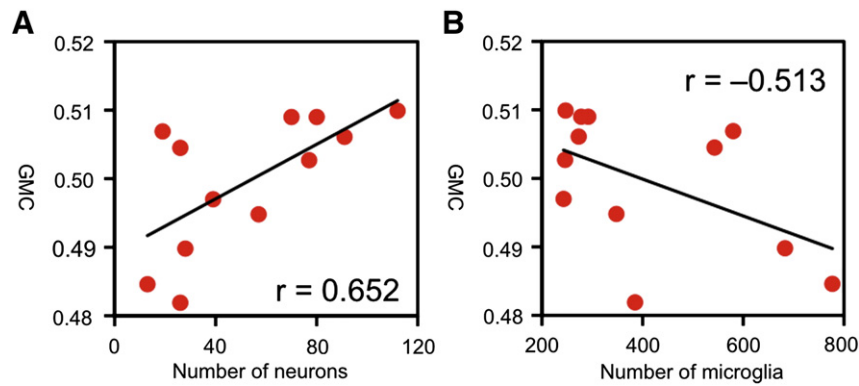


Fig. 5. The correlations between GMC values and the numbers of neurons (A) or microglia (B) in CA1 of CPR rats. CA1, CA1 region of the hippocampus; CPR, cardiopulmonary resuscitation; GMC, gray matter concentration.

The number of neurons and microglia in CA1 are expressed as the mean \pm standard error of mean (SEM) and were analyzed using Student's *t*-tests at a significance level of $P < 0.05$. To investigate whether VBM-detected gray matter changes are associated with hippocampal damage, a correlation analysis (Pearson test) was applied to the mean gray matter probability values inside the ROI and the number of neurons or microglia in CA1. A correlation analysis was also performed between the number of neurons and microglia. Because CPR rats exhibited significant changes in GMC and in the numbers of neurons and microglia compared to sham-operated controls, correlation analyses were only performed in CPR rats to avoid biasing the correlation. The significance level of all correlation analyses was set at $P < 0.05$. All statistical tests were two-tailed.

Results

VBM

To support the first hypothesis, VBM successfully revealed significant regional decreases in GMC and GMV in CPR rats compared to sham-operated controls in brain regions, including CA1. The region in which a significant decrease in GMC was localized to CA1 (Supplementary Figs. 1A, B), whereas reductions in GMV extended throughout the entire hippocampus (Supplementary Figs. 1C, D) ($P < 0.05$ FWE corrected). The restriction of GMC decrease to CA1 was consistent even with the less significant threshold at $P < 0.05$ FDR corrected (Figs. 3A, B). Similar to other studies of CPR in rats (Katz et al., 1995; Keilhoff et al., 2010, 2011; Shoykhet et al., 2012), local neuronal loss and microglial invasion were observed in CA1 in CPR rats but not in sham-operated controls (Figs. 3E–J). Thus, the region in which a significant decrease in GMC was observed (CA1) coincided with the same region that exhibited neuronal loss and microglial invasion in response to CPR. In contrast, the analysis of GMV detected not only CA1 but also the other hippocampal regions where the histological differences were not obvious between sham-operated controls and CPR rats. These results indicated that both the analyses of GMC and GMV were sensitive but the analysis of GMC was more specific to the CPR-induced histological abnormalities in CA1 as compared with the analysis of GMV.

Association between VBM and hippocampal damage

Quantifications of the number of immunopositive cells revealed a significant decrease in neuronal number and an increase in microglial number in CA1 in CPR rats compared to sham-operated controls (Figs. 4B, C). Thus, we observed a significant negative correlation between the number of neurons and the number of microglia in CPR rats ($r = -0.777$, $P = 0.003$, Fig. 4D). This effect likely resulted from the fact that microglial invasion in CA1 is involved in the

inflammatory cascades that accompany neuronal cell death due to cardiac arrest and subsequent CPR (Keilhoff et al., 2010, 2011).

As shown in Fig. 3, both the GMC decrease and histological abnormalities were localized to CA1. Thus, the probability values inside the GMC decrease detected by VBM (GMC values) were compared with the number of neurons or microglia in CA1. To support the second hypothesis, we observed a significant positive correlation between GMC values and the number of neurons ($r = 0.652$, $P = 0.021$, Fig. 5A) and a trend towards a negative correlation between GMC values and the number of microglia ($r = -0.513$, $P = 0.088$, Fig. 5B) in CA1 of CPR rats. Therefore, VBM-detected changes in gray matter were associated with hippocampal damage in CPR rats. Thus, it appears that VBM-detected alterations in gray matter can be used as a surrogate marker for hippocampal damage following CPR.

Discussions

In the present study, we compared the VBM data directly with neuronal and microglial cell counts in CA1 of the same CPR rat brains. The reason why we use VBM, which identifies regional differences in the concentration or volume of a particular tissue such as gray matter (Ashburner and Friston, 2000, 2001), in the present study is that CPR-induced histological abnormalities occur exclusively in a gray matter region (CA1). The major findings of the present study were as follows: (1) VBM successfully revealed regional GMC and GMV decreases in the brain regions, including CA1, in CPR rats compared to sham-operated controls, (2) the decrease in GMC was localized to CA1, which is the same brain region that exhibited neuronal loss and microglial invasion in CPR rats, and (3) there was a significant positive correlation between GMC values and the number of neurons and a trend towards a negative correlation between GMC values and the number of microglia in CA1 of CPR rats. These findings indicate that VBM-detected alterations in gray matter can be used as a surrogate marker for hippocampal damage in CPR rats.

VBM-detected alterations in gray matter in CPR rats compared to sham-operated controls

In the present study, VBM revealed regional decreases in GMC and GMV in the hippocampus in CPR rats compared to sham-operated controls. Neuronal loss and microglial invasion in CA1 were observed in CPR rats but not in sham-operated controls. Similarly, previous studies have shown that survivors after CPR exhibit decreases in gray matter that can be detected by VBM (Horstmann et al., 2010) and exhibit neuronal loss (Cummings et al., 1984; Press et al., 1989; Volpe and Petito, 1985; Zola-Morgan et al., 1986) in the hippocampus. However, a previous research has also reported decreases in gray matter in other cortical and subcortical regions that were also observed in CPR survivors (Horstmann et al., 2010). This discrepancy

may be explained by the fact that CA1 is particularly sensitive to ischemia that results from asphyxia-induced cardiac arrest compared to other brain regions, such as the cortex, caudate putamen, thalamus, and cerebellum in rats (Katz et al., 1995).

The present study revealed that the decrease in GMC was observed exclusively in CA1, which exhibited neuronal loss and microglial invasion in response to CPR. In contrast, the analysis of GMV detected not only CA1 but also the other hippocampal regions where the histological differences were not obvious between CPR rats and sham-operated controls. These results indicated that both the analyses of GMC and GMV were sensitive but the analysis of GMC was more specific to the CPR-induced histological abnormalities in CA1 as compared with the analysis of GMV. The detection of larger regions exhibiting changes in GMV than those in GMC is consistent with the results from a previous VBM study in patients with epilepsy (Keller et al., 2004) and could possibly be explained by brain tissue deformation that is similarly observed in space-occupying lesions or surgical resection of tissue (Liu et al., 2006). Such deformation of CA3 and dentate gyrus could potentially be detected more effectively by the modulation step of GMV analysis on hippocampal normalization, which preserves the variability in local tissue morphology (Good et al., 2001; Keller et al., 2004; Mechelli et al., 2005).

The association between VBM and hippocampal damage in CPR rats

In the present study, GMC values were observed to be significantly and positively correlated with the number of neurons and tended to be negatively correlated with the number of microglia in CA1 of CPR rats. There are several potential explanations for this observed association between GMC values and hippocampal damage. First, changes in the number of neurons and glia may affect relaxation time and hence voxel intensities, which reflect gray matter probability (Zatorre et al., 2012). In contrast, the temporal lobes resected from patients with epilepsy showed no significant correlations between gray matter probability values and neuronal or astrocyte density (Eriksson et al., 2009; Lockwood-Estrin et al., 2012). Second, damage to neuron-associated structures, such as axons, dendrites, and synapses, may induce the changes in gray matter observed in CPR rats. Axonal remodeling, dendritic branching, and synaptogenesis have been proposed to contribute to increases in gray matter that have been reported during exercise and learning (May, 2011; Zatorre et al., 2012). In a deformation-based morphometry study in mice, MRI volume changes induced by water maze training have been shown to be correlated with the expression of a marker of axonal remodeling (Lerch et al., 2011). Exposing rodents to an enriched environment has also been shown to increase gray matter volume, dendritic length, and synaptic numbers, despite not leading to any changes in the number of neurons (Anderson, 2011). Third, abnormalities in the extracellular space that result from hippocampal damage could contribute to the observed changes in gray matter in CPR rats. In infarcted brain regions, the apparent diffusion coefficient (ADC) values in diffusion-weighted MRIs decrease in the acute phase before gradually normalizing and increasing in the chronic phase. This ADC effect can be partially explained by extracellular changes that affect water mobility (Marks et al., 1996; Provenzale and Sorensen, 1999). Widespread decreases in ADC values were also observed after cardiac arrest (Mlynash et al., 2010; Wijman et al., 2009). Consistent with these reports, it is possible that a combination of the aforementioned cellular and extracellular events associated with hippocampal damage affect the GMC values in CPR rats.

Limitations of the present study

The present study had limitations. First, certain gray matter regions such as the thalamus were misclassified as white matter in the probabilistic maps of the population specific template in the present study. This classification error occurred in the unified segmentation process, and

was also observed in the Wistar rat brain template (Valdés-Hernández et al., 2011). The probabilistic images of the Wistar rat brain were segmented from native MRI images by using a histogram analysis, which probably caused the misclassification of the thalamus. The anatomical segmentation of mice brain MRI images was also associated with difficulties in defining several brain structures and anatomical borders (Ma et al., 2005, 2008). However, the misclassification might not affect the VBM results of the present study because the hippocampus was properly classified as gray matter. Second, cardiac arrest was induced by asphyxia in the present study. In contrast, cardiac arrest in patients occurs primarily as a result of ventricular fibrillation (VF) or tachycardia (VT) (Bayés de Luna et al., 1989; Wood et al., 1994). There is also a rat model of cardiac arrest induced by VF (Knapp et al., 2011; von Planta et al., 1988) that also results in neuronal degeneration of CA1 (Knapp et al., 2011), an effect that is similar to that observed in rats with asphyxia-induced cardiac arrest (Katz et al., 1995; Keilhoff et al., 2010, 2011; Shoykhet et al., 2012). Therefore, the VBM results of asphyxia-induced cardiac arrest in the present study are likely relevant for those of VF-induced cardiac arrest in rats.

Conclusions

The present study demonstrated that VBM-detected alterations in gray matter can be used as a surrogate marker for hippocampal damage following CPR.

Acknowledgments

The authors would like to thank Ms. Yumi Watanabe and Chika Miyamoto for their assistance with histological preparations and analyses. In addition, we would like to thank Mr. Hiroi Nonaka for his technical assistance and Tohoku University International Advanced Research and Education Organization for supporting our research.

Conflict of interest

There is no conflict of interest in this study.

Appendix A. Supplementary data

Supplementary data to this article can be found online at <http://dx.doi.org/10.1016/j.neuroimage.2013.03.042>.

References

- Anderson, B.J., 2011. Plasticity of gray matter volume: the cellular and synaptic plasticity that underlies volumetric change. *Dev. Psychobiol.* 53, 456–465.
- Ashburner, J., 2007. A fast diffeomorphic image registration algorithm. *Neuroimage* 38, 95–113.
- Ashburner, J., Friston, K.J., 2000. Voxel-based morphometry – the methods. *Neuroimage* 11, 805–821.
- Ashburner, J., Friston, K.J., 2001. Why voxel-based morphometry should be used. *Neuroimage* 14, 1238–1243.
- Ashburner, J., Friston, K.J., 2005. Unified segmentation. *Neuroimage* 26, 839–851.
- Bayés de Luna, A., Coumel, P., Leclercq, J.F., 1989. Ambulatory sudden cardiac death: mechanisms of production of fatal arrhythmia on the basis of data from 157 cases. *Am. Heart J.* 117, 151–159.
- Biedermann, S., Fuss, J., Zheng, L., Sartorius, A., Falfán-Melgoza, C., Demirakca, T., Gass, P., Ende, G., Weber-Fahr, W., 2012. In vivo voxel based morphometry: detection of increased hippocampal volume and decreased glutamate levels in exercising mice. *Neuroimage* 61, 1206–1212.
- Cummings, J.L., Tomiyasu, U., Read, S., Benson, D.F., 1984. Amnesia with hippocampal lesions after cardiopulmonary arrest. *Neurology* 34, 679–681.
- Empey, P.E., Miller, T.M., Philbrick, A.H., Melick, J.A., Kochanek, P.M., Poloyac, S.M., 2012. Mild hypothermia decreases fentanyl and midazolam steady-state clearance in a rat model of cardiac arrest. *Crit. Care Med.* 40, 1221–1228.
- Eriksson, S.H., Free, S.L., Thom, M., Symms, M.R., Martinian, L., Duncan, J.S., Sisodiya, S.M., 2009. Quantitative gray matter histological measures do not correlate with gray matter probability values from in vivo MRI in the temporal lobe. *J. Neurosci. Methods* 181, 111–118.

- Good, C.D., Johnsrude, I.S., Ashburner, J., Henson, R.N.A., Friston, K.J., Frackowiak, R.S.J., 2001. A voxel-based morphometric study of ageing in 465 normal adult human brains. *Neuroimage* 14, 21–36.
- Horstmann, A., Frisch, S., Jentzsch, R.T., Müller, K., Villringer, A., Schroeter, M.L., 2010. Resuscitating the heart but losing the brain: brain atrophy in the aftermath of cardiac arrest. *Neurology* 74, 306–312.
- Katz, L., Ebmeyer, U., Safar, P., Radovsky, A., Neumar, R., 1995. Outcome model of asphyxial cardiac arrest in rats. *J. Cereb. Blood Flow Metab.* 15, 1032–1039.
- Keilhoff, G., John, R., Langnaese, K., Schweizer, H., Ebmeyer, U., 2010. Triggered by asphyxia neurogenesis seems not to be an endogenous repair mechanism, gliogenesis more like it. *Neuroscience* 171, 869–884.
- Keilhoff, G., Schweizer, H., John, R., Langnaese, K., Ebmeyer, U., 2011. Minocycline neuroprotection in a rat model of asphyxial cardiac arrest is limited. *Resuscitation* 82, 341–349.
- Keller, S.S., Wilke, M., Wiesmann, U.C., Sluming, V.A., Roberts, N., 2004. Comparison of standard and optimized voxel-based morphometry for analysis of brain changes associated with temporal lobe epilepsy. *Neuroimage* 23, 860–868.
- Klein, A., Andersson, J., Ardekani, B.A., Ashburner, J., Avants, B., Chiang, M.C., Christensen, G.E., Collins, D.L., Gee, J., Hellier, P., Song, J.H., Jenkinson, M., Lepage, C., Rueckert, D., Thompson, P., Vercauteren, T., Woods, R.P., Mann, J.J., Parsey, R.V., 2009. Evaluation of 14 nonlinear deformation algorithms applied to human brain MRI registration. *Neuroimage* 46, 786–802.
- Knapp, J., Heinzmann, A., Schneider, A., Padosch, S.A., Böttiger, B.W., Teschendorf, P., Popp, E., 2011. Hypothermia and neuroprotection by sulfide after cardiac arrest and cardiopulmonary resuscitation. *Resuscitation* 82, 1076–1080.
- Lerch, J.P., Yiu, A.P., Martinez-Canabal, A., Pekar, T., Bohbot, V.D., Frankland, P.W., Henkelman, R.M., Josselyn, S.A., Sled, J.G., 2011. Maze training in mice induces MRI-detectable brain shape changes specific to the type of learning. *Neuroimage* 54, 2086–2095.
- Lim, C., Alexander, M.P., LaFleche, G., Schnyer, D.M., Verfaellie, M., 2004. The neurological and cognitive sequelae of cardiac arrest. *Neurology* 63, 1774–1778.
- Liu, Y., D'Arceuil, H., He, J., Duggan, M., Gonzalez, G., Pryor, J., de Crespigny, A., 2006. A nonlinear mesh-warping technique for correcting brain deformation after stroke. *Magn. Reson. Imaging* 24, 1069–1075.
- Liu, H., Sarnaik, S.M., Manole, M.D., Chen, Y., Shinde, S.N., Li, W., Rose, M., Alexander, H., Chen, J., Clark, R.S., Graham, S.H., Hickey, R.W., 2012. Increased cytochrome c in rat cerebrospinal fluid after cardiac arrest and its effects on hypoxic neuronal survival. *Resuscitation* 83, 1491–1496.
- Lockwood-Estrin, G., Thom, M., Focke, N.K., Symms, M.R., Martinian, L., Sisodiya, S.M., Duncan, J.S., Eriksson, S.H., 2012. Correlating 3 T MRI and histopathology in patients undergoing epilepsy surgery. *J. Neurosci. Methods* 205, 182–189.
- Ma, Y., Hof, P.R., Grant, S.C., Blackband, S.J., Bennett, R., Slatest, L., McGuigan, M.D., Benveniste, H., 2005. A three-dimensional digital atlas database of the adult C57BL/6J mouse brain by magnetic resonance microscopy. *Neuroscience* 135, 1203–1205.
- Ma, Y., Smith, D., Hof, P.R., Foerster, B., Hamilton, S., Blackband, S.J., Yu, M., Benveniste, H., 2008. *Front. Neuroanat.* 2, 1–10.
- Marks, M.P., de Crespigny, A., Lentz, D., Enzmann, D.R., Albers, G.W., Moseley, M.E., 1996. Acute and chronic stroke: navigated spin-echo diffusion-weighted MR imaging. *Radiology* 199, 403–408.
- Mateen, F.J., Josephs, K.A., Trenerry, M.R., Felmler-Devine, M.D., Weaver, A.L., Carone, M., White, R.D., 2011. Long-term cognitive outcomes following out-of-hospital cardiac arrest: a population-based study. *Neurology* 77, 1438–1445.
- May, A., 2011. Experience-dependent structural plasticity in the adult human brain. *Trends Cogn. Sci.* 15, 475–482.
- May, A., Hajak, G., Gänssbauer, S., Steffens, T., Langguth, B., Kleinjung, T., Eichhammer, P., 2007. Structural brain alterations following 5 days of intervention: dynamic aspects of neuroplasticity. *Cereb. Cortex* 17, 205–210.
- Mechelli, A., Price, C.J., Friston, K.J., Ashburner, J., 2005. Voxel-based morphometry of the human brain: methods and applications. *Curr. Med. Imaging Rev.* 1, 1–9.
- Mlynash, M., Campbell, D.M., Leproust, E.M., Fischbein, N.J., Bammer, R., Eyngorn, I., Hsia, A.W., Moseley, M., Wijman, C.A., 2010. Temporal and spatial profile of brain diffusion-weighted MRI after cardiac arrest. *Stroke* 41, 1665–1672.
- Press, G.A., Amaral, D.G., Squire, L.R., 1989. Hippocampal abnormalities in amnesic patients revealed by high-resolution magnetic resonance imaging. *Nature* 341, 54–57.
- Provenzale, J.M., Sorensen, A.G., 1999. Diffusion-weighted MR imaging in acute stroke: theoretic considerations and clinical applications. *Am. J. Roentgenol.* 173, 1459–1467.
- Quallo, M.M., Price, C.J., Ueno, K., Asamizuya, T., Cheng, K., Lemon, R.N., Iriki, A., 2009. Gray and white matter changes associated with tool-use learning in macaque monkeys. *Proc. Natl. Acad. Sci. U.S.A.* 106, 18379–18384.
- Roine, R.O., Kajaste, S., Kaste, M., 1993. Neuropsychological sequelae of cardiac arrest. *JAMA* 269, 237–242.
- Sawiak, S.J., Wood, N.I., Williams, G.B., Morton, A.J., Carpenter, T.A., 2009. Voxel-based morphometry in the R6/2 transgenic mouse reveals differences between genotypes not seen with manual 2D morphometry. *Neurobiol. Dis.* 33, 20–27.
- Shoykhet, M., Simons, D.J., Alexander, H., Hosler, C., Kochanek, P.M., Clark, R.S., 2012. Thalamocortical dysfunction and thalamic injury after asphyxial cardiac arrest in developing rats. *J. Neurosci.* 32, 4972–4981.
- Sumiyoshi, A., Suzuki, H., Ogawa, T., Riera, J.J., Shimokawa, H., Kawashima, R., 2012. Coupling between gamma oscillation and fMRI signal in the rat somatosensory cortex: its dependence on systemic physiological parameters. *Neuroimage* 60, 738–746.
- Taguchi, N., Nakayama, S., Tanaka, M., 2012. Fluoxetine has neuroprotective effects after cardiac arrest and cardiopulmonary resuscitation in mouse. *Resuscitation* 83, 652–656.
- Taki, Y., Hashizume, H., Thyreau, B., Sassa, Y., Takeuchi, H., Wu, K., Kotozaki, Y., Nouchi, R., Asano, M., Asano, K., Fukuda, H., Kawashima, R., 2012. Sleep duration during weekdays affects hippocampal gray matter volume in healthy children. *Neuroimage* 60, 471–475.
- Valdés-Hernández, P.A., Sumiyoshi, A., Nonaka, H., Haga, R., Vasquez, E.A., Ogawa, T., Medina, Y.I., Riera, J.J., Kawashima, R., 2011. An in vivo MRI template set for morphometry, tissue segmentation and fMRI localization in rats. *Front. Neuroinform.* 5, 26.
- Volpe, B.T., Petito, C.K., 1985. Dementia with bilateral medial temporal lobe ischemia. *Neurology* 35, 1793–1797.
- Von Planta, I., Weil, M.H., von Planta, M., Bisera, J., Bruno, S., Gazmuri, R.J., Rackow, E.C., 1988. Cardiopulmonary resuscitation in the rat. *J. Appl. Physiol.* 65, 2641–2647.
- Wijman, C.A., Mlynash, M., Caulfield, A.F., Hsia, A.W., Eyngorn, I., Bammer, R., Fischbein, N., Albers, G.W., Moseley, M., 2009. Prognostic value of brain diffusion-weighted imaging after cardiac arrest. *Ann. Neurol.* 65, 394–402.
- Wood, M.A., Stambler, B.S., Damiano, R.J., Greenway, P., Ellenbogen, K.A., 1994. Lessons learned from data logging in a multicenter clinical trial using a late-generation implantable cardioverter-defibrillator. The Guardian ATP 4210 Multicenter Investigators Group. *J. Am. Coll. Cardiol.* 24, 1692–1699.
- Yang, J., Wadghiri, Y.Z., Hoang, D.M., Tsui, W., Sun, Y., Chung, E., Li, Y., Wang, A., de Leon, M., Wisniewski, T., 2011. Detection of amyloid plaques targeted by USPIO-A β 1–42 in Alzheimer's disease transgenic mice using magnetic resonance microimaging. *Neuroimage* 55, 1600–1609.
- Zatorre, R.J., Fields, R.D., Johansen-Berg, H., 2012. Plasticity in gray and white: neuroimaging changes in brain structure during learning. *Nat. Neurosci.* 15, 528–536.
- Zhang, X., Salmeron, B.J., Ross, T.J., Geng, X., Yang, Y., Stein, E.A., 2011. Factors underlying prefrontal and insula structural alterations in smokers. *Neuroimage* 54, 42–48.
- Zola-Morgan, S., Squire, L.R., Amaral, D.G., 1986. Human amnesia and the medial temporal region: enduring memory impairment following a bilateral lesion limited to field CA1 of the hippocampus. *J. Neurosci.* 6, 2950–2967.